

Supplemental Data Summary

Supplementary Figure S1: Supplementary Figure S1 shows the fluorescence imaging dynamics of AR9.6-IRDye800 in a Colo357 subcutaneous xenograft model.

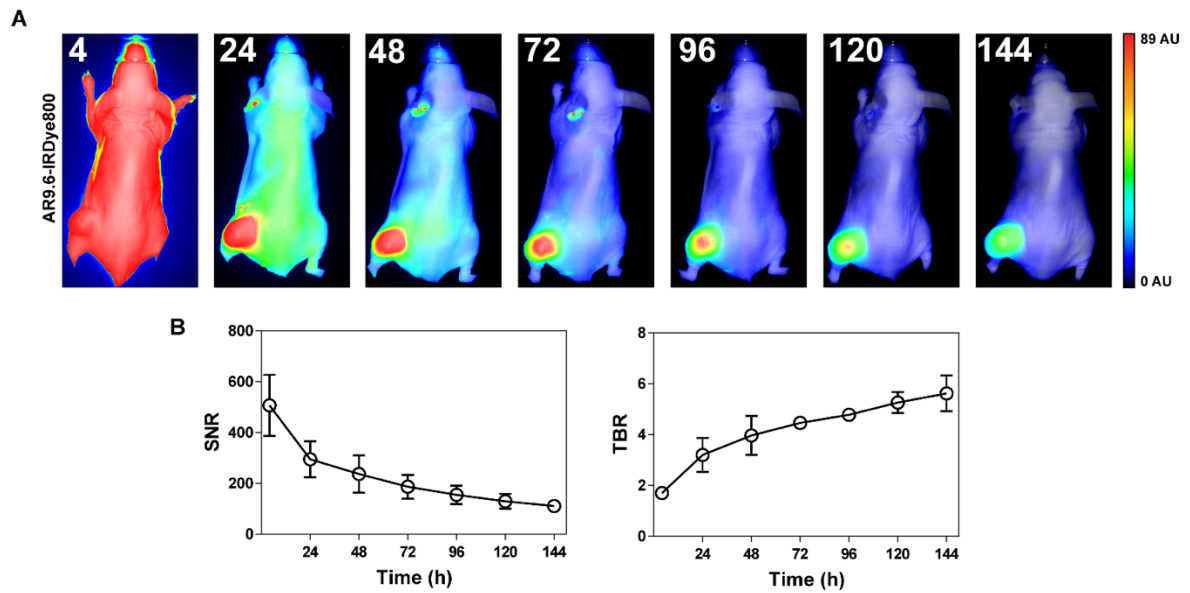
Supplementary Figure S2: Supplementary Figure S2 shows the biodistribution of fluorescent conjugates in subcutaneous xenografts at 144 h post-injection.

Supplementary Figure S3: Supplementary Figure S3 shows the internalization of AR9.6-IRDye800 *in vitro*.

Supplementary Video S1: Supplementary Video S1 shows surgical resection with AR9.6-IRDye800.

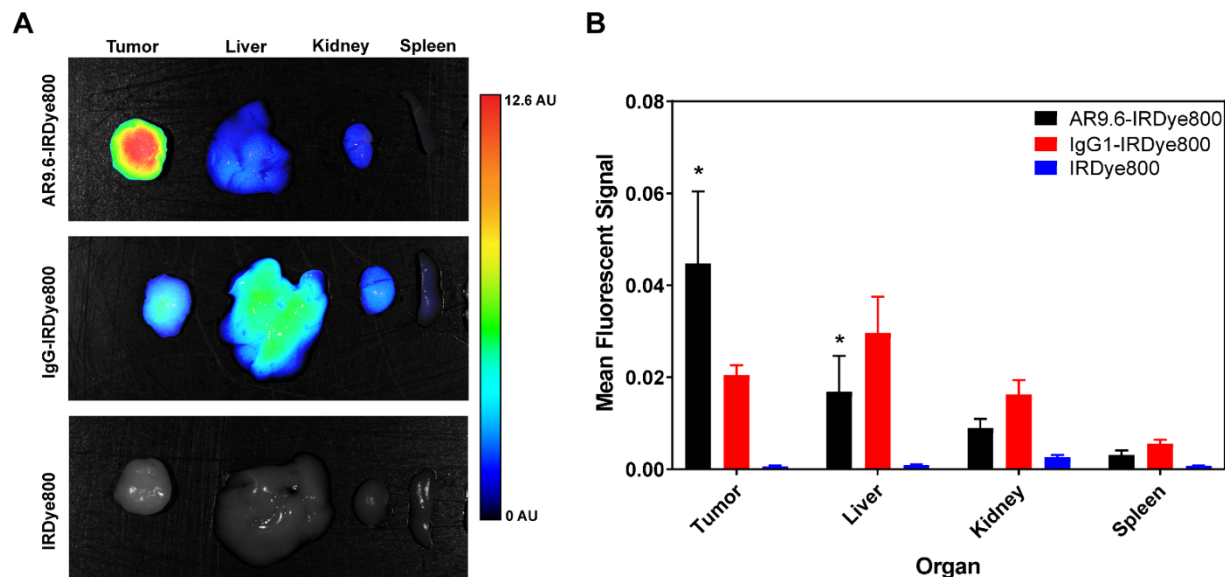
Supplementary Video S2: Supplementary Video S2 shows surgical resection with IgG-IRDye800.

Supplementary Data:



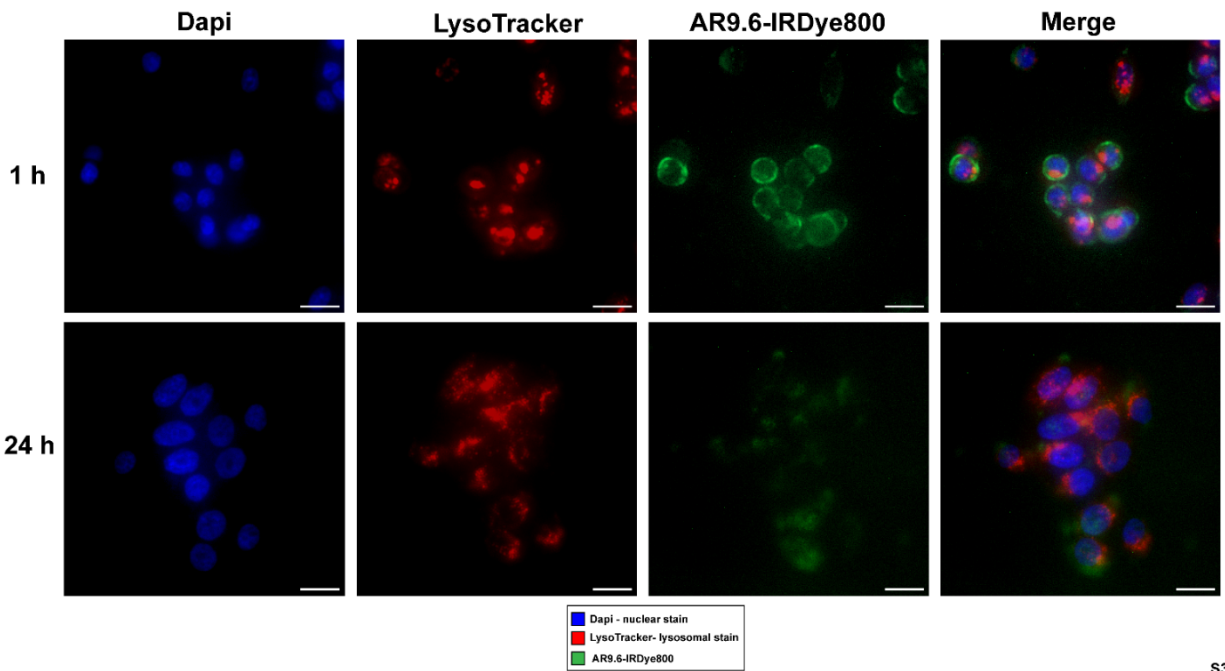
S1

Supplemental Figure S1. Biodistribution of AR9.6 in a Colo357 subcutaneous xenograft model over 144 h. (A) Representative images from LI-COR Pearl imaging, images on color bar scaled to arbitrary units (AU). (B) Tumor signal to noise ratio (SNR) and tumor to background ratio (TBR) over 144 h ($N=4$).



S2

Supplemental Figure S2. (A). Biodistribution of AR9.6-IRDye800, IgG-IRDye800, and unconjugated IRDye800 in key clearance organs at 144 h in subcutaneous T3M4 model from optimal imaging time study. Color bar scaled to normalized arbitrary units for all images. (B) Mean fluorescent signal in key clearance organs at 144 h ($N=4$). Significance determined by Two way ANOVA, followed by Tukey's test for multiple comparisons. Tumor to tumor comparison: $p < 0.0001$ for AR9.6-IRDye800 compared to IgG-IRDye800 and IRDye800. Tumor to liver comparison: $p < 0.0085$ for AR9.6-IRDye800 compared to IgGIRDye800, and $p < 0.009$ for AR9.6-IRDye800 compared to IRDye800.



S3

Supplemental Figure S3. Internalization of AR9.6-IRDye800 at 1 hour and 24 hours after incubation.

Supplemental Video S1. Surgical resection of AR9.6-IRDye800 with Fluobeam imaging system.

Supplemental Video S2. Surgical resection of IgG-IRDye800 with Fluobeam imaging system.